

Including screening in van-der-Waals corrected DFT calculations. The case of atoms and small molecules physisorbed on graphene

Pier Luigi Silvestrelli

Dipartimento di Fisica e Astronomia, Università di Padova,

via Marzolo 8, I-35131, Padova, Italy,

and DEMOCRITOS National Simulation Center,

of the Italian Istituto Officina dei Materiali (IOM) of the

Italian National Research Council (CNR), Trieste, Italy

Abstract

The DFT/vdW-QHO-WF method, recently developed to include the van der Waals (vdW) interactions in approximated Density Functional Theory (DFT) by combining the Quantum Harmonic Oscillator model with the Maximally Localized Wannier Function technique, is applied to the cases of atoms and small molecules (X=Ar, CO, H₂, H₂O) weakly interacting with benzene and with the ideal planar graphene surface. Comparison is also presented with the results obtained by other DFT vdW-corrected schemes, including PBE+D, vdW-DF, vdW-DF2, rVV10, and by the simpler Local Density Approximation (LDA) and semilocal Generalized Gradient Approximation (GGA) approaches. While for the X-benzene systems all the considered vdW-corrected schemes perform reasonably well, it turns out that an accurate description of the X-graphene interaction requires a proper treatment of many-body contributions and of short-range screening effects, as demonstrated by adopting an improved version of the DFT/vdW-QHO-WF method. We also comment on the widespread attitude of relying on LDA to get a rough description of weakly interacting systems.

I. INTRODUCTION

Nowadays the importance of graphene both from a theoretical point of view and considering the ever growing interest for many possible nanotechnology applications cannot be surely overemphasized.¹⁻³ Of particular relevance is the investigation of isolated molecules interacting with graphene. In fact, for instance, the operational principle of graphene devices is mainly based on changes in their electrical conductivity due to gas molecules adsorbed on the graphene surface.¹ The study of the interactions of graphene with water is also very important as a model for the characterization of the interface between water and hydrophobic substrates,⁴ and considering the recently reported application of graphene as an atomically flat coating for atomic force microscopy used for investigating the growth of water adlayers on a substrate.⁵ In addition, a single water molecule adsorbed on graphene represents a weakly interacting system involving a complex mixture of Hydrogen bonding, electrostatic, and van der Waals interactions, thus providing a significant test model for any electronic structure theory.⁶

Moreover, observations indicate that the cold regions of the interstellar medium contain clouds made of atoms, radicals and simple, “astrobiological” molecules such as H_2 , CO, H_2O ,..., as well as small solids typically composed of amorphous water, silicates and carbon grains in the form of graphite, amorphous structures and polycyclic aromatic hydrocarbon molecules, such as benzene.⁷ More complex molecules are probably formed by surface-catalysed chemical reactions on low temperatures interstellar dust grains. Clearly a pre-requisite for describing such processes is the possibility of accurately reproducing the interactions between isolated small molecules and grain-surface models.

Carbon-based nanomaterials have also attracted much attention because of their suitability as materials for gas storage. In particular, the reported high hydrogen uptake of these materials make them attractive for hydrogen storage devices in fuel-cell-powered electric vehicles.⁸ Among the available carbon nano-materials, the graphene sheet is the simplest one and may store hydrogen on both side of its structure. The hydrogen-storage process implies the H atomic chemisorption after the dissociation of the H_2 molecules, so that elucidating the H_2 molecular physisorption stage that precedes the dissociation is clearly very important.⁹

In view of the above considerations we have decided to investigate the interaction of

atoms and small molecules (X=Ar, CO, H₂, H₂O) with benzene and with the ideal planar graphene surface, by adopting the most recent theoretical approaches based on the Density Functional Theory (DFT), explicitly developed to describe dispersion, van der Waals (vdW) interactions neglected¹⁰ in standard DFT calculations, and thus being able to reproduce even weak physisorption processes. In particular, the interactions of Ar and H₂ with benzene and graphene are representative of purely dispersion binding, while those involving CO and H₂O are typical examples of mixed (dispersion/electrostatic and also Hydrogen-bond for H₂O) interactions: in fact the polar water molecule is characterized by a substantial dipole moment, while the weakly polar CO molecule behaves as an electric quadrupole.⁷

In the last few years several practical methods have been proposed to make DFT calculations able to accurately describe vdW effects (for a recent review, see, for instance, refs. 11–13). We have developed a family of such methods, all based on the generation of the Maximally Localized Wannier Functions (MLWFs),¹⁴ successfully applied to a variety of systems, including small molecules, water clusters, graphite and graphene, water layers interacting with graphite, interfacial water on semiconducting substrates, hydrogenated carbon nanotubes, molecular solids, the interaction of rare gases and small molecules with metal surfaces,... For the sake of clarity in the following we briefly summarize the evolutionary process of these methods by reporting the improvements which have been implemented during the time, together with the adopted nomenclature:

DFT/vdW-WF denotes the original scheme^{6,9,15–21} where the vdW correction to the binding energy is obtained by using the basic information (center positions and spreads) given by the MLWFs and the functional proposed by Andersson, Langreth, and Lundqvist (see eq. (10) of ref. 22) to evaluate the C_6 coefficients that characterize the long-range interaction between two separated fragments of matter. The DFT/vdW-WF method has been independently improved by Andrinopoulos *et al.*²³ to consider partly occupied Wannier functions and p -like states.

The subsequent DFT/vdW-WF2 version²⁴ is based on the simpler London expression and takes into account the intrafragment overlap of the localized Wannier functions, leading to a considerable improvement in the evaluation of the C_6 vdW coefficients.

DFT/vdW-WF2s²⁵ indicates a modification of DFT/vdW-WF2 to take metal-screening effects into account to be applied to the study of adsorption of rare gases and small molecules on metal surfaces.

Finally, the latest DFT/vdW-QHO-WF method²⁶ combines the Quantum Harmonic Oscillator (QHO) model with the MLWFs, in such a way to be no longer restricted to the case of well separated interacting fragments and to include higher than pairwise energy contributions, coming from the dipole–dipole coupling among quantum oscillators. In the specific case of adsorption on metal surfaces a long-range damping factor has been introduced²⁶ to take metal-screening effects into account.

Here we apply the DFT/vdW-QHO-WF approach to investigate atoms and small molecules weakly interacting with benzene and with the ideal planar graphene surface. Our results will be compared to the best available, reference experimental and theoretical values, and to those obtained by other DFT vdW-corrected schemes, including PBE+D,²⁷ vdW-DF,^{28,29} vdW-DF2,³⁰ rVV10,³¹ and by the simpler Local Density Approximation (LDA) and semilocal Generalized Gradient Approximation (GGA, in the PBE flavor³²) approaches. In the PBE+D scheme DFT calculations at the PBE level are corrected by adding empirical C_6/R^6 potentials with parameters determined by fitting accurate energies for a large molecular database, while in the vdW-DF, vdW-DF2, and rVV10 methods vdW effects are included by introducing DFT non-local correlation functionals. While for the X-benzene systems both DFT/vdW-QHO-WF and the other considered vdW-corrected schemes perform well, it turns out that an accurate description of the X-graphene interaction requires a proper treatment of many-body contributions and of short-range screening effects, so that modified versions of the DFT/vdW-QHO-WF method are introduced and their performance is assessed.

II. METHOD

Here we briefly review the DFT/vdW-QHO-WF method; additional details can be found in ref. 26.

For a system of N three-dimensional QHOs the exact total energy can be obtained^{33–37} by diagonalizing the $3N \times 3N$ matrix C^{QHO} , containing N^2 blocks C_{ij}^{QHO} of size 3×3 :

$$C_{ii}^{QHO} = \omega_i^2 \mathbf{I} \quad ; \quad C_{i \neq j}^{QHO} = \omega_i \omega_j \sqrt{\alpha_i \alpha_j} T_{ij} \quad (1)$$

where \mathbf{I} is the identity matrix, T_{ij} is the dipole-dipole interaction tensor, and ω_i and α_i are the characteristic frequency and the static dipole polarizability, respectively, of the

i -th oscillator. The interaction (correlation) energy is given by the difference between the ground state energy of the *coupled* system of QHOs (proportional to the square root of the eigenvalues λ_p of the C^{QHO} matrix) and the ground state energy of the *uncoupled* system of QHOs (derived from the characteristic frequencies):

$$E_{c,QHO} = 1/2 \sum_{p=1}^{3N} \sqrt{\lambda_p} - 3/2 \sum_{i=1}^N \omega_i. \quad (2)$$

The so-computed interaction energy naturally includes many body energy contributions, due to the dipole–dipole coupling among the QHOs; moreover, it can be proved³⁷ that the QHO model provides an efficient description of the correlation energy for a set of localized fluctuating dipoles at an effective Random Phase Approximation (RPA)-level. This is important because, differently from other schemes, RPA includes the effects of long-range screening of the vdW interactions,³⁸ which are clearly of relevance, particularly for extended systems.^{13,39,40}

The QHO model can be combined with the MLWF technique by assuming that each MLWF is represented by a three-dimensional isotropic harmonic oscillator, so that the system is described as an assembly of fluctuating dipoles. By considering³⁷ the Coulomb interaction between two spherical Gaussian charge densities to account for orbital overlap at short distances (thus introducing a short-range damping):

$$V_{ij} = \frac{\text{erf}(r_{ij}/\sigma_{ij})}{r_{ij}}, \quad (3)$$

where r_{ij} is the distance between the i -th and the j -th Wannier Function Center (WFC), and σ_{ij} is an effective width, $\sigma_{ij} = \sqrt{S_i^2 + S_j^2}$, where S_i is the spread of the i -th MLWF. Then, in Eq. (1) the dipole interaction tensor is³⁷

$$T_{ij}^{ab} = -\frac{3r_{ij}^a r_{ij}^b - r_{ij}^2 \delta_{ab}}{r_{ij}^5} \left(\text{erf}\left(\frac{r_{ij}}{\sigma_{ij}}\right) - \frac{2}{\sqrt{\pi}} \frac{r_{ij}}{\sigma_{ij}} e^{-\left(\frac{r_{ij}}{\sigma_{ij}}\right)^2} \right) + \frac{4}{\sqrt{\pi}} \frac{1}{\sigma_{ij}^3} \frac{r_{ij}^a r_{ij}^b}{r_{ij}^2} e^{-\left(\frac{r_{ij}}{\sigma_{ij}}\right)^2} \quad (4)$$

where a and b specify Cartesian coordinates (x, y, z), r_{ij}^a and r_{ij}^b are the respective components of the distance r_{ij} , and δ_{ab} is the Kronecker delta function.

Moreover, as in ref. 24, adopting a simple classical theory, the polarizability of an electronic shell of charge eZ_i and mass mZ_i , tied to a heavy undeformable ion, is written as

$$\alpha_i = \zeta \frac{Z_i e^2}{m \omega_i^2}. \quad (5)$$

Then, given the direct relation between polarizability and volume,⁴¹ we assume that $\alpha_i = \gamma S_i^3$, where γ is a proportionality constant, so that the orbital volume is expressed in terms of the i -th MLWF spread, S_i .

Similarly to ref. 37, we combine the QHO model, which accurately describes the long-range correlation energy, with a given semilocal, Generalized Gradient Approximation (GGA) functional (PBE in our case), which is expected to well reproduce short-range correlation effects, by introducing an empirical parameter β that multiplies the QHO-QHO parameter σ_{ij} in Eq. (3). The three parameters β , γ , and ζ are set up by minimizing the mean absolute relative errors (MARE), measured with respect to high-level, quantum-chemistry reference values relative to the S22 database of intermolecular interactions,⁴² a widely used benchmark database, consisting of weakly interacting molecules (a set of 22 weakly interacting dimers mostly of biological importance), with reference binding energies calculated by a number of different groups using high-level quantum chemical methods. By taking PBE as the reference DFT functional, we get: $\beta = 1.39$, $\gamma = 0.88$, and $\zeta = 1.30$.²⁶ Once the γ and ζ parameters are set up, both the polarizability α_i and the characteristic frequency ω_i are obtained just in terms of the MLWF spreads (see Eq. (5) and below).

As anticipated above, the DFT/vdW-QHO-WF scheme can be improved to achieve a better description of screening effects. In fact the presence of the environment acts to screen the dipolar fluctuations and both short- and long-range effects should be properly included. As a first choice we follow the strategy proposed in ref. 35, where the frequency-dependent polarizability tensor of finite-gap molecules and solids is obtained by using the self-consistent screening (SCS) equation of classical electrodynamics:

$$\alpha_{ab}^{SCS}(\mathbf{r}, i\omega) = \alpha_{ab}(\mathbf{r}, i\omega) + \sum_{cd} \alpha_{ac}(\mathbf{r}, i\omega) \int d\mathbf{r}' U_{cd}(\mathbf{r} - \mathbf{r}') \alpha_{db}^{SCS}(\mathbf{r}', i\omega). \quad (6)$$

Since our MLWFs are represented as a collection of isotropic QHOs (differently from ref. 35, where the atoms of the system were described as QHOs) the above equation can be discretized as follows :

$$\alpha_{i,ab}^{SCS} = \alpha_{i,ab} + \sum_{cd} \alpha_{i,ac} \sum_{j \neq i} U_{ij,cd} \alpha_{j,db}^{SCS}, \quad (7)$$

where the tensor U is related to the dipole interaction tensor defined above : $U_{ij,ab} = -T_{ij}^{ab}$.

Then, starting from an isotropic polarizability (see above) :

$$\alpha_{i,ab} = \alpha_i \delta_{ab} = \gamma S_i^3 , \quad (8)$$

by focusing on the isotropic contribution of the SCS polarizability only, one obtains :

$$\alpha_i^{SCS} = 1/3 \sum_a \alpha_{i,aa}^{SCS} , \quad (9)$$

where :

$$\begin{aligned} \alpha_{i,aa}^{SCS} &= \alpha_i + \alpha_i \sum_{j \neq i} \sum_c U_{ij,ac} \alpha_{j,ca}^{SCS} = \\ &= \alpha_i + \alpha_i \sum_{j \neq i} U_{ij,aa} \alpha_{j,aa}^{SCS} + \alpha_i \sum_{j \neq i} \sum_{c \neq a} U_{ij,ac} \alpha_{j,ca}^{SCS} = \\ &= \alpha_i + \alpha_i \sum_{j \neq i} U_{ij,aa} \alpha_{j,aa}^{SCS} + \mathcal{O}(U^2) . \end{aligned}$$

We have explicitly checked, that neglecting the $\mathcal{O}(U^2)$ terms in the above expression, has negligible effects (less than 0.1 meV in the binding energy for all the systems considered in the present study), so that one can safely use the simpler, approximated expression:

$$\alpha_{i,aa}^{SCS} \simeq \alpha_i + \alpha_i \sum_{j \neq i} U_{ij,aa} \alpha_{j,aa}^{SCS} , \quad (10)$$

representing a system of linear equations which can be easily solved by a matrix inversion:

$$\alpha_{i,aa}^{SCS} = \sum_j (A_a^{-1})_{ij} \alpha_j , \quad (11)$$

where :

$$(A_a)_{ii} = 1 , \quad (A_a)_{ij} = -\alpha_i U_{ij,aa} \quad (j \neq i) . \quad (12)$$

The isotropic, SCS polarizability α_i^{SCS} then replace the original polarizability α_i in the matrix C^{QHO} of Eq. (1). We denote the version of our method modified by SCS effects as DFT/vdW-QHO-WF-SCS.

Additional investigations⁴³ suggested that, within the QHO model, a better treatment of screening effects can be accomplished by range-separating the U interaction tensor into a short and a long-range component: the short-range (SR) component is used for the short-range SCS of the polarizabilities, while the long-range (LR) one is used in the QHO Hamiltonian. In this way no double counting of long-range screening effects is present,⁴³ which represents an advantage with respect to the SCS method described above, especially in highly anisotropic systems, where the long-range effects tend to dominate over the short-range screening. In practice, this new scheme is implemented as follows :

(i) the SCS procedure is only restricted to SR :

$$\alpha_{i,aa}^{SCS} = \alpha_i + \alpha_i \sum_{j \neq i} U_{ij,aa}^{SR} \alpha_{j,aa}^{SCS} , \quad (13)$$

where $U_{ij,aa}^{SR} = (1 - f_{ij,aa})U_{ij,aa}$, $f_{ij,aa}$ being a suitable range-separating damping function; (ii) in Eq. (1) the dipole-dipole interaction tensor is replaced by its LR component :

$$T_{ij}^{abLR} = f_{ij,ab} T_{ij}^{ab} . \quad (14)$$

In ref. 43 the range separation is enforced by introducing a Fermi-type function, depending on an empirical parameter to be fitted on minimizing the mean absolute relative error for a reference database. In the present approach we have instead adopted an alternative expression for the damping function, namely :

$$f_{ij,ab} = U_{ij,ab} / D_{ij,ab} , \quad (15)$$

with the constraint that $f_{ij,ab}$ is set to zero if the above expression leads to a negative (unphysical) value; here $D_{ij,ab}$ indicates the U interaction tensor at large distances :

$$D_{ij}^{ab} = \frac{3r_{ij}^a r_{ij}^b - r_{ij}^2 \delta_{ab}}{r_{ij}^5} . \quad (16)$$

This expression has the advantage that no additional empirical parameter is added. Moreover, extensive testing show that it is more suited to our approach where the QHOs mimic the MLWFs instead of the atoms as in ref. 43. This new scheme, which is basically characterized by restricting the SCS procedure to short-range interactions only, will be referred to as DFT/vdW-QHO-WF-SCS-SR.

The calculations have been performed with both the CPMD⁴⁴ and the Quantum-ESPRESSO ab initio package⁴⁵ (in the latter case the MLWFs have been generated as a post-processing calculation using the WanT package⁴⁶). Electron-ion interactions were described using norm-conserving pseudopotentials and the PBE reference DFT functional³² which was adopted also in refs. 26,37 and represents one of the most popular GGA choices. In our calculations graphene was modeled using a supercell containing 72 C atoms (similarly to what assumed in previous theoretical studies^{4,6}), in such a way to prevent the X fragment from interacting with its periodic images, and an empty region of about 15 Å width was left among the graphene replicas, in the direction orthogonal to the graphene plane. The in-plane geometry was fixed to the one determined experimentally (C–C distance = 1.421 Å). The sampling of the Brillouin Zone was limited to the Γ point, again as done in previous studies.^{4,6}

In all the cases the X atom or molecule has been placed above the center of the benzene ring or of a Carbon hexagon of graphene (in agreement with the favored configurations suggested by previous studies) and the distance between the X fragment and the benzene or graphene plane has been optimized. In the case of X=H₂ and X=H₂O the molecule is orthogonal to the plane (with the H atoms pointing downwards for water), while for X=CO the molecule is parallel, again in agreement with previous findings (see references listed in the Result section and in the related tables).

Although in principle the values of the three parameters β , γ , and ζ introduced above could be reoptimized as the new DFT/vdW-QHO-WF-SCS and DFT/vdW-QHO-WF-SCS-SR schemes are applied, we have maintained their original values (namely at the DFT/vdW-QHO-WF level) both because in this way the effects of the SCS and SCS-SR corrections can be more clearly assessed, and also because a reoptimization using the S22 database (consisting of interacting molecules) as the reference set would be of doubtful utility since here our primary interest is the application to extended systems such as those involving graphene.

III. RESULTS AND DISCUSSION

In Tables I and II we report the binding energy and the equilibrium distance for X-benzene and X-graphene systems, respectively. These quantities have been computed using the

DFT/vdW-QHO, DFT/vdW-QHO-SCS, and DFT/vdW-QHO-SCS-SR methods described above, but also a variety of other vdW-corrected schemes, including PBE+D, vdW-DF, vdW-DF2, rVV10, and the simpler (non-vdW-corrected) LDA and semilocal GGA (in the PBE flavor) approaches.

As can be seen looking at Table I, for the X-benzene systems all the considered vdW-corrected methods perform reasonably well. In more detail, with respect to the DFT/vdW-QHO scheme, DFT/vdW-QHO-SCS reduces the binding energy and increases the equilibrium distance, while DFT/vdW-QHO-SCS-SR gives intermediate results. On the whole DFT/vdW-QHO-SCS-SR clearly better reproduces the binding energy, while the same is not evident for the equilibrium distance, also considering that the reference values are affected by a significant uncertainty.

Concerning the other schemes, rVV10, whose performances are comparable to those of DFT/vdW-QHO-SCS-SR, seems to give the best results. As already pointed out in the literature,^{16,29} the vdW-DF method, based on the revPBE GGA functional,⁴⁷ clearly overestimates the equilibrium distances; moreover, it turns out that vdW-DF2 represents a significant improvement with respect to the previous vdW-DF scheme, particularly concerning the equilibrium distances. Not surprisingly the performances of the non-vdW-corrected LDA and PBE methods are very poor, with LDA (PBE) which severely overestimates (underestimates) the binding energies and underestimates (overestimates) the equilibrium distances, thus indicating that for the systems we have investigated a proper inclusion of vdW effects is crucial.

Coming to the calculations on X-graphene (see Table II), the general trend is similar to that observed for X-benzene, however, important differences can be noticed. In particular, interesting quantities to look at, are represented by the ratios between the value of the binding energy and of the equilibrium distance relative to an X-graphene system and that of the corresponding X-benzene system (see Table III). One can observe that, for the binding energy, using the LDA and PBE methods, the ratio is considerably lower than that between the best available, reference experimental and theoretical values (last two rows of Table III), thus indicating that these non-vdW-corrected schemes are not able to properly describe long-range interactions characterizing the weak binding between atoms/molecules and graphene. Clearly, only adopting vdW-corrected methods one can recover these effects.

As far as the equilibrium distances are concerned, one can see that, going from X-benzene

to X-graphene systems, their behavior is not simply correlated to the that of the corresponding binding energies, namely it is not necessarily true that a decrease in the binding energy leads to an increase in the equilibrium distances; actually, most of the distances slightly decrease from X-benzene to X-graphene, but for X=H₂O where the equilibrium distance is almost unchanged.

As a way to assess the performances of the different schemes in a more quantitative way, in Tables IV and V we report the Mean Absolute Relative Error of the computed binding energy, MARE_e , and of the equilibrium distance, MARE_d , together with their sum, MARE_s , by computing the error relative to the reference theoretical values (when multiple reference data are available average values have been considered). The MARE_e for both X-benzene and X-graphene systems is also shown in Fig. 1. Of course these quantities can only be viewed as rough quantitative indicators, also considering that the reference values are often quite scattered (as, for instance, in the case of water interacting with graphene), nonetheless they convey the basic information. To facilitate the performance assessment, in Tables IV and V, we have listed the different methods in the order of decreasing MARE_s . As can be expected, the pure-GGA PBE method performance is poor, as the result of a dramatic underbinding and strong overestimate of the equilibrium distances. Clearly the DFT/vdW-QHO-SCS-SR schemes performs well and represents an evident improvement with respect to the previous DFT/vdW-QHO approach (and also to the DFT/vdW-QHO-SCS variant). Interestingly, for the X-benzene systems DFT/vdW-QHO-SCS-SR is second only to rVV10, while for the X-graphene it gives the best results, thus suggesting that it gives a better description of screening in extended systems. In fact, vdW-DF, vdW-DF2, and rVV10 tend to overestimate the binding energy ratio (see Table III); this effect can be probably ascribed to the neglect of long-range screening effects by these methods.^{13,38} Therefore one can conclude that, while for the X-benzene systems all the considered vdW-corrected schemes perform reasonably well (the MARE_e of PBE+D, vdW-DF2, rVV10, and DFT/vdW-QHO-SCS-SR is not larger than 15%), it turns out that an accurate description of the X-graphene interaction requires a proper treatment of many-body contributions and of both long- and short-range screening effects: in fact with PBE+D, vdW-DF2, and rVV10 the MARE_e is larger than 17%, and reduces to less than 10% only with DFT/vdW-QHO-SCS-SR. Quite interestingly, the worsening of the performances which characterize all the methods in going from X-benzene to X-graphene systems, is much reduced (it is the smallest)

with DFT/vdW-QHO-SCS-SR.

The LDA performances deserve a separate comment, since, looking at Tables IV and V (see also Fig. 1), it appears that, while for X-benzene systems the LDA results are very poor, for X-graphene they are almost comparable to those of vdW-corrected schemes and are much better than those obtained by PBE. This could lead to adopt a simple LDA approach in order to get a rough description of graphene/graphite weakly interacting with small fragments. However these relatively good LDA performances should not be overemphasized, because they are the just the result of a cancellation of errors: in fact LDA tends to overestimate the binding energy in small systems (see Tables I and IV), that is at short and medium range (in particular the exchange contribution is overestimated⁴⁸), while, in extended systems, it is not able to proper describe long-range correlation effects, which are therefore dramatically underestimated. Moreover, the common assumption⁴⁹ that LDA always tends to overbinding in systems where vdW interactions are important, so that the LDA value provides an upper limit to the (absolute value of) the binding energy, can be misleading, as demonstrated (see Table II) by the Ar-graphene case where LDA turns out to underestimate the interaction energy. In addition one must point out that with LDA the equilibrium distances are always significantly underestimated.

IV. CONCLUSIONS

In conclusion, we have presented an improved version of the DFT/vdW-QHO-WF method, recently proposed to include the vdW interactions in DFT, that has been specifically developed to better describe short-range screening effects. The new scheme has been applied to atoms and small molecules interacting with benzene and with the ideal planar graphene surface. The computed binding energies and equilibrium distances have been compared with those obtained by the original DFT/vdW-QHO-WF method and by other vdW-corrected schemes, showing that the new DFT/vdW-QHO-SCS-SR approach represents a clear improvement with respect to DFT/vdW-QHO-WF and, particularly in the description of X-graphene systems, outperforms the other methods, thus indicating that in extended systems a proper treatment of both many-body contributions and of long- and short-range screening effects is essential. Finally, the simple LDA approach, which performs much better than the semilocal PBE GGA, seems to offer a reasonable description of X-

graphene systems, in line with previous observations,⁴⁸ although one should always be aware of the intrinsic limitations of the method.

V. ACKNOWLEDGEMENTS

We thank very much R. Sabatini for help in performing rVV10 calculations and A. Ambrosetti for useful discussions.

-
- ¹ K. S. Novoselov *et al.*, Science **306**, 666 (2004); A. K. Geim, K. S. Novoselov, Nature Mater. **6**, 183 (2007); F. Schedin *et al.*, Nature Mater. **6**, 652 (2007).
 - ² M. Vanin, J. J. Mortensen, A. K. Kelkkanen, J. M. Garcia-Lastra, K. S. Thygesen, and K. W. Jacobsen, Phys. Rev. B **81**, 081408(R) (2010) and references therein.
 - ³ K. S. Kim *et al.*, Nature **457**, 706 (2009).
 - ⁴ M. Rubeš, P. Nachtigall, J. Vondrášek, O. Bludský, J. Phys. Chem. C **113**, 8412 (2009).
 - ⁵ K. Xu, P. Cao, J. R. Heath, Science **329**, 1188 (2010).
 - ⁶ A. Ambrosetti, P. L. Silvestrelli, J. Phys. Chem. C **115**, 3695 (2011).
 - ⁷ A. Lakhlif, J. P. Killingbeck, Surf. Sci. **604**, 38 (2010).
 - ⁸ A. K. Geim, Science **324**, 1530 (2009).
 - ⁹ F. Costanzo, P. L. Silvestrelli, Francesco Ancilotto, J. Chem. Theory Comp. **8**, 1288 (2012); Archives of Metallurgy and Materials **57**, 1075 (2012).
 - ¹⁰ See, for instance, W. Kohn, Y. Meir, D. E. Makarov, Phys. Rev. Lett. **80**, 4153 (1998).
 - ¹¹ K. E. Riley, M. Pitoňák, P. Jurečka, P. Hobza, Chem. Rev. **110**, 5023 (2010).
 - ¹² A. Tkatchenko, L. Romaner, O. T. Hofmann, E. Zojer, C. Ambrosch-Draxl, and M. Scheffler, MRS Bulletin, **35**, 435 (2010).
 - ¹³ J. Klimeš, A. Michaelides, J. Chem. Phys. **137**, 120901 (2012).
 - ¹⁴ N. Marzari and D. Vanderbilt, Phys. Rev. B **56**, 12847 (1997).
 - ¹⁵ P. L. Silvestrelli, Phys. Rev. Lett **100**, 053002 (2008).
 - ¹⁶ P. L. Silvestrelli, J. Phys. Chem. A **113**, 5224 (2009).
 - ¹⁷ P. L. Silvestrelli, K. Benyahia, S. Grubisić, F. Ancilotto, F. Toigo, J. Chem. Phys. **130**, 074702 (2009).

- ¹⁸ P. L. Silvestrelli, *Chem. Phys. Lett.* **475**, 285 (2009).
- ¹⁹ P. L. Silvestrelli, F. Toigo, F. Ancilotto, *J. Phys. Chem. C* **113**, 17124 (2009).
- ²⁰ P. L. Silvestrelli, A. Ambrosetti, S. Grubisić, and F. Ancilotto, *Phys. Rev. B* **85**, 165405 (2012).
- ²¹ A. Ambrosetti, F. Ancilotto, P. L. Silvestrelli, *J. Phys. Chem. C* **117**, 321 (2013).
- ²² Y. Andersson, D. C. Langreth, and B. I. Lundqvist, *Phys. Rev. Lett.* **76**, 102 (1996).
- ²³ L. Andrinopoulos, N. D. M. Hine, A. A. Mostofi, *J. Chem. Phys.* **135**, 154105 (2011).
- ²⁴ A. Ambrosetti, P. L. Silvestrelli, *Phys. Rev. B* **85**, 073101 (2012).
- ²⁵ P. L. Silvestrelli and A. Ambrosetti, *Phys. Rev. B* **87**, 075401 (2013).
- ²⁶ P. L. Silvestrelli, *J. Chem. Phys.* **139**, 054106 (2013).
- ²⁷ S. Grimme, *J. Comp. Chem.* **27**, 1787 (2006); V. Barone, M. Casarin, D. Forrer, M. Pavone, M. Sambi, A. Vittadini, *J. Comp. Chem.* **30**, 934 (2009).
- ²⁸ M. Dion, H. Rydberg, E. Schröder, D. C. Langreth, B. I. Lundqvist, *Phys. Rev. Lett.* **92**, 246401 (2004); G. Roman-Perez, J. M. Soler, *Phys. Rev. Lett.* **103**, 096102 (2009).
- ²⁹ T. Thonhauser, V. R. Cooper, S. Li, A. Puzder, P. Hyldgaard, D. C. Langreth, *Phys. Rev. B* **76**, 125112 (2007).
- ³⁰ K. Lee, É. D. Murray, L. Kong, B. I. Lundqvist, and D. C. Langreth, *Phys. Rev. B* **82**, 081101(R) (2010).
- ³¹ R. Sabatini, T. Gorni, S. de Gironcoli, *Phys. Rev. B* **87**, 041108(R) (2013).
- ³² J. P. Perdew, K. Burke, M. Ernzerhof, *Phys. Rev. Lett.* **77**, 3865 (1996).
- ³³ J. Cao, B. J. Berne, *J. Chem. Phys.* **97**, 8628 (1992).
- ³⁴ A. G. Donchev, *J. Chem. Phys.* **125**, 074713 (2006).
- ³⁵ A. Tkatchenko, R. A. Di Stasio, R. Car, M. Scheffler, *Phys. Rev. Lett.* **108**, 236402 (2012).
- ³⁶ A. M. Reilly, A. Tkatchenko, *J. Phys. Chem. Lett.* **4**, 1028 (2013).
- ³⁷ A. Tkatchenko, A. Ambrosetti, R. A. Di Stasio Jr., *J. Chem. Phys.* **138**, 074106 (2013).
- ³⁸ F. Göttl, A. Grünesi, T. Bučko, J. Hafner, *J. Chem. Phys.* **137**, 114111 (2012).
- ³⁹ T. Bučko, S. Lebègue, J. Hafner, J. G. Ángyán, *Phys. Rev. B* **87**, 064110 (2013).
- ⁴⁰ A. Tkatchenko, D. Alfé, K. S. Kim, *J. Chem. Theory Comput.* **8**, 4317 (2012).
- ⁴¹ T. Brink, J. S. Murray, P. Politzer, *J. Chem. Phys.* **98**, 4305 (1993).
- ⁴² P. Jurečka, J. Šponer, J. Černý, P. Hobza, *Phys. Chem. Chem. Phys.* **8**, 1985 (2006).
- ⁴³ A. Ambrosetti, A. Reilly, R. Di Stasio Jr., A. Tkatchenko, preprint (2013) arXiv:1312.3806.
- ⁴⁴ See www.cpmid.org for information about the CPMD package.

- ⁴⁵ See www.quantum-espresso.org for information about the Quantum-ESPRESSO package.
- ⁴⁶ See www.wannier-transport.org for information about the WanT package; see also: A. Calzolari, N. Marzari, I. Souza and M. Buongiorno Nardelli, *Phys. Rev. B* **69**, 035108 (2004).
- ⁴⁷ Y. Zhang, W. Yang, *Phys. Rev. Lett.* **80**, 890 (1998).
- ⁴⁸ K. Berland, S. D. Chakarova-Käck, V. R. Cooper, D. C. Langreth, E. Schröder, *J. Phys.: Condens. Matter* **23**, 135001 (2011).
- ⁴⁹ X. Lin, J. Ni, C. Fang, *J. Appl. Phys.* **113**, 034306 (2013).
- ⁵⁰ Th. Brupbacher, J. Makarewicz, A. Bauder, *J. Chem. Phys.* **101**, 9736 (1994).
- ⁵¹ H. Koch, B. Fernández, O. Christiansen, *J. Chem. Phys.* **108**, 2784 (1998).
- ⁵² D. L. Crittenden, *J. Phys. Chem. A* **113**, 1663 (2009).
- ⁵³ A. G. Donchev, *J. Chem. Phys.* **126**, 124706 (2007).
- ⁵⁴ O. Hübner, A. Glöss, M. Fichtner, W. Klopp, *J. Phys. Chem. A* **108**, 3019 (2004).
- ⁵⁵ S. Hamel, M. Cô, *J. Chem. Phys.* **121**, 12618 (2004).
- ⁵⁶ R. Nowak, J. A. Menapace, E. R. Bernstein, *J. Chem. Phys.* **89**, 1309 (1988).
- ⁵⁷ Th. Brupbacher, A. Bauder, *J. Chem. Phys.* **99**, 9394 (1993).
- ⁵⁸ P. I. Nagy, C. W. Ulmer, D. A. Smith, *J. Chem. Phys.* **102**, 6812 (1995).
- ⁵⁹ B. P. Stoicheff, *Can. J. Phys.* **32**, 339 (1954).
- ⁶⁰ A. J. Gotch, T. S. Zwier, *J. Chem. Phys.* **96**, 3388 (1992).
- ⁶¹ B.-M. Cheng, J. R. Grover, E. A. Walters, *Chem. Phys. Lett.* **232**, 364 (1995).
- ⁶² Y. Zhao, O. Tishchenko, D. G. Truhlar, *J. Phys. Chem. B* **109**, 19046 (2005).
- ⁶³ S. K. Min, E. C. Lee, H. M. Lee, D. Y. Kim, D. Kim, K. S. Kim, *J. Comput. Chem.* **29**, 1208 (2008).
- ⁶⁴ L. F. Molnar, X. He, B. Wang, K. M. Merz Jr., *J. Chem. Phys.* **131**, 065102 (2009).
- ⁶⁵ G. Vidali, G. Ihm, H. Y. Kim, M. W. Cole, *Surf. Sci. Rep.* **12**, 135 (1991).
- ⁶⁶ A. Tkatchenko, O. A. Lilienfeld, *Phys. Rev. B* **73**, 153406 (2006).
- ⁶⁷ L. Mattera, F. Rosatelli, C. Salvo, F. Tommasini, U. Valbusa, G. Vidali, *Surf. Sci.* **93**, 515 (1980).
- ⁶⁸ M. Rubeš, O. Bludský, *Chem. Phys. Chem.* **10**, 1868 (2009).
- ⁶⁹ J. Piper, J. A. Morrison, C. Peters, *Mol. Phys.* **53**, 1463 (1984).
- ⁷⁰ Y.-H. Zhang, Y.-B. Chen, K.-G. Zhou, C.-H. Liu, J. Zeng, H.-L. Zhang, Y. Peng, *Nanotechnology* **20**, 185504 (2009).

- ⁷¹ N. N. Avgul, A. V. Kieslev, *Chem. Phys. Carbon* **6**, 1 (1970).
- ⁷² G. R. Jenness, O. Karalti, K. D. Jordan, *Phys. Chem. Chem. Phys.* **12**, 6375 (2010).
- ⁷³ J. Kysilka, M. Rubeš, L. Grajciar, P. Nachtigall, O. Bludský, *J. Phys. Chem. A* **115**, 11387 (2011).
- ⁷⁴ E. Voloshina, D. Usvyat, M. Schütz, Y. Dedkov, B. Paulus, *Phys. Chem. Chem. Phys.* **13**, 12041 (2011).
- ⁷⁵ J. Ma, A. Michaelides, D. Alfé, L. Schimka, G. Kresse, E. Wang, *Phys. Rev. B* **84**, 033402 (2011).
- ⁷⁶ X. Li, J. Feng, E. Wang, S. Meng, J. Klimees, A. Michaelides, *Phys. Rev. B* **85**, 085425 (2012).
- ⁷⁷ I. Hamada, *Phys. Rev. B* **86**, 195436 (2012).

TABLE I: Binding energy E_b (in meV) and (in parenthesis) equilibrium distance R (in Å) for X-benzene systems, using different methods, compared with available experimental and theoretical reference data. R is defined as the separation between Ar, (the closest) H, C, and O atoms, and the benzene plane, for X=Ar, X=H₂, X=CO, and X=H₂O, respectively.

method	X=Ar	X=H ₂	X=CO	X=H ₂ O
LDA	-74[3.24]	-101[2.40]	-153[3.09]	-222[3.03]
PBE	-11[3.90]	-21[2.94]	-25[3.68]	-84[3.46]
PBE+D	-50[3.50]	-58[2.57]	-77[3.19]	-172[3.18]
vdW-DF	-64[3.72]	-45[3.15]	-86[3.56]	-122[3.60]
vdW-DF2	-57[3.58]	-45[2.90]	-85[3.44]	-129[3.47]
rVV10	-51[3.51]	-46[2.72]	-85[3.23]	-147[3.31]
DFT/vdW-QHO	-63[3.53]	-45[2.75]	-95[3.31]	-152[3.27]
DFT/vdW-QHO-SCS	-41[3.67]	-40[2.86]	-62[3.47]	-120[3.38]
DFT/vdW-QHO-SCS-SR	-51[3.66]	-38[2.90]	-78[3.44]	-133[3.36]
ref. expt.	-51[3.50] ^a	—	-76[3.24,3.44] ^{g,h}	-141±12[3.32±0.07] ^{j,k,l}
ref. theory	-50↔-48[3.55] ^{b,c}	-55↔-40[2.70] ^{d,e,f}	-77[3.32] ⁱ	-142±5[3.35] ^{c,m,n,o}

^aref.50.

^bref.51.

^cref.52.

^dref.53.

^eref.54.

^fref.55.

^gref.56.

^href.57.

ⁱref.58.

^jref.59.

^kref.60.

^lref.61.

^mref.62.

ⁿref.63.

^oref.64.

TABLE II: Binding energy E_b (in meV) and (in parenthesis) equilibrium distance R (in Å) for X-graphene systems, using different methods, compared with available experimental and theoretical reference data. R is defined as the separation between Ar, (the closest) H, C, and O atoms, and the graphene plane, for X=Ar, X=H₂, X=CO, and X=H₂O, respectively. When reference data for X-graphene were not available, the corresponding values relative to X-graphite have been reported, which probably slightly overestimate^{4,6} the binding energy with graphene, since graphite can be considered as an assembly of multiple graphene layers.

method	X=Ar	X=H ₂	X=CO	X=H ₂ O
LDA	-84[3.16]	-86[2.40]	-110[3.03]	-146[3.06]
PBE	-13[3.85]	-13[3.05]	-12[3.72]	-28[3.65]
PBE+D	-95[3.33]	-66[2.53]	-106[3.18]	-147[3.17]
vdW-DF	-137[3.54]	-77[2.98]	-160[3.47]	-140[3.64]
vdW-DF2	-113[3.41]	-67[2.80]	-144[3.29]	-129[3.36]
rVV10	-112[3.34]	-64[2.65]	-149[3.17]	-140[3.25]
DFT/vdW-QHO	-136[3.34]	-50[2.75]	-147[3.21]	-137[3.26]
DFT/vdW-QHO-SCS	-88[3.45]	-41[2.86]	-85[3.35]	-91[3.37]
DFT/vdW-QHO-SCS-SR	-112[3.49]	-40[2.86]	-117[3.36]	-113[3.38]
ref. expt.	-99±4[3.0±0.1] ^a	-48[—] ^c	-113±1[—] ^e	-156[—] ^h
ref. theory	-116[3.33] ^b	-56[2.58] ^d	-120[3.02] ^f , -112[3.0] ^g	-140↔-72[3.26↔3.46] ^{g,i,k,l,m,n,o}

^aref.65 (on graphite).

^bref.66 (on graphite).

^cref.67 (on graphite).

^dref.68.

^eref.69 (on graphite).

^fref.70.

^gref.49.

^href.71 (on graphite).

ⁱref.4.

^jref.72.

^kref.73.

^lref.74.

^mref.75.

ⁿref.76.

^oref.77.

TABLE III: Binding energy and equilibrium distance (in parenthesis) ratio between the value relative to an X-graphene system and that of the corresponding X-benzene system. When multiple reference data are available, ratios between average values have been considered. The last column reports values averaged over the four X fragments.

method	X=Ar	X=H ₂	X=CO	X=H ₂ O	average
LDA	1.14[0.98]	0.85[1.00]	0.72[0.98]	0.66[1.01]	0.84[0.99]
PBE	1.18[0.99]	0.62[1.04]	0.48[1.01]	0.33[1.05]	0.65[1.02]
PBE+D	1.90[0.95]	1.14[0.98]	1.38[1.00]	0.85[1.00]	1.32[0.98]
vdW-DF	2.14[0.95]	1.71[0.95]	1.86[0.97]	1.15[1.01]	1.71[0.97]
vdW-DF2	1.98[0.95]	1.49[0.97]	1.69[0.96]	1.00[0.97]	1.54[0.96]
rVV10	2.30[0.95]	1.39[0.97]	1.75[0.98]	0.95[0.98]	1.60[0.97]
DFT/vdW-QHO	2.16[0.95]	1.11[1.00]	1.55[0.97]	0.90[1.00]	1.43[0.98]
DFT/vdW-QHO-SCS	2.15[0.94]	1.02[1.00]	1.37[0.97]	0.76[1.00]	1.32[0.98]
DFT/vdW-QHO-SCS-SR	2.20[0.95]	1.05[0.99]	1.50[0.98]	0.85[1.01]	1.40[0.98]
ref. expt.	1.94[0.86]	— [—]	1.49[—]	1.11[—]	—
ref. theory	2.37[0.94]	1.18[0.96]	1.51[0.93]	0.75[1.00]	1.45[0.96]

TABLE IV: Mean absolute relative error of computed binding energy, MARE_e , and equilibrium distance, MARE_d , together with their sum, MARE_s , relative to X-benzene systems.

method	$\text{MARE}_e(\%)$	$\text{MARE}_d(\%)$	$\text{MARE}_s(\%)$
LDA	80.2	9.1	89.3
PBE	60.3	8.2	68.5
vdW-DF	15.2	9.0	24.2
DFT/vdW-QHO-SCS	16.5	3.7	20.2
DFT/vdW-QHO	15.8	1.3	17.1
PBE+D	11.6	3.8	15.4
vdW-DF2	10.0	3.9	13.9
DFT/vdW-QHO-SCS-SR	7.7	3.6	11.3
rVV10	5.0	1.4	6.4

TABLE V: Mean absolute relative error of computed binding energy, MARE_e , and equilibrium distance, MARE_d , together with their sum, MARE_s , relative to X-graphene systems.

method	$\text{MARE}_e(\%)$	$\text{MARE}_d(\%)$	$\text{MARE}_s(\%)$
PBE	82.2	16.5	98.7
vdW-DF	30.9	11.4	42.3
LDA	31.0	5.4	36.4
DFT/vdW-QHO-SCS	22.9	6.5	29.4
DFT/vdW-QHO	21.0	4.1	25.1
PBE+D	20.8	3.3	24.1
rVV10	20.0	2.9	22.9
vdW-DF2	17.0	5.1	22.1
DFT/vdW-QHO-SCS-SR	9.9	7.0	16.9

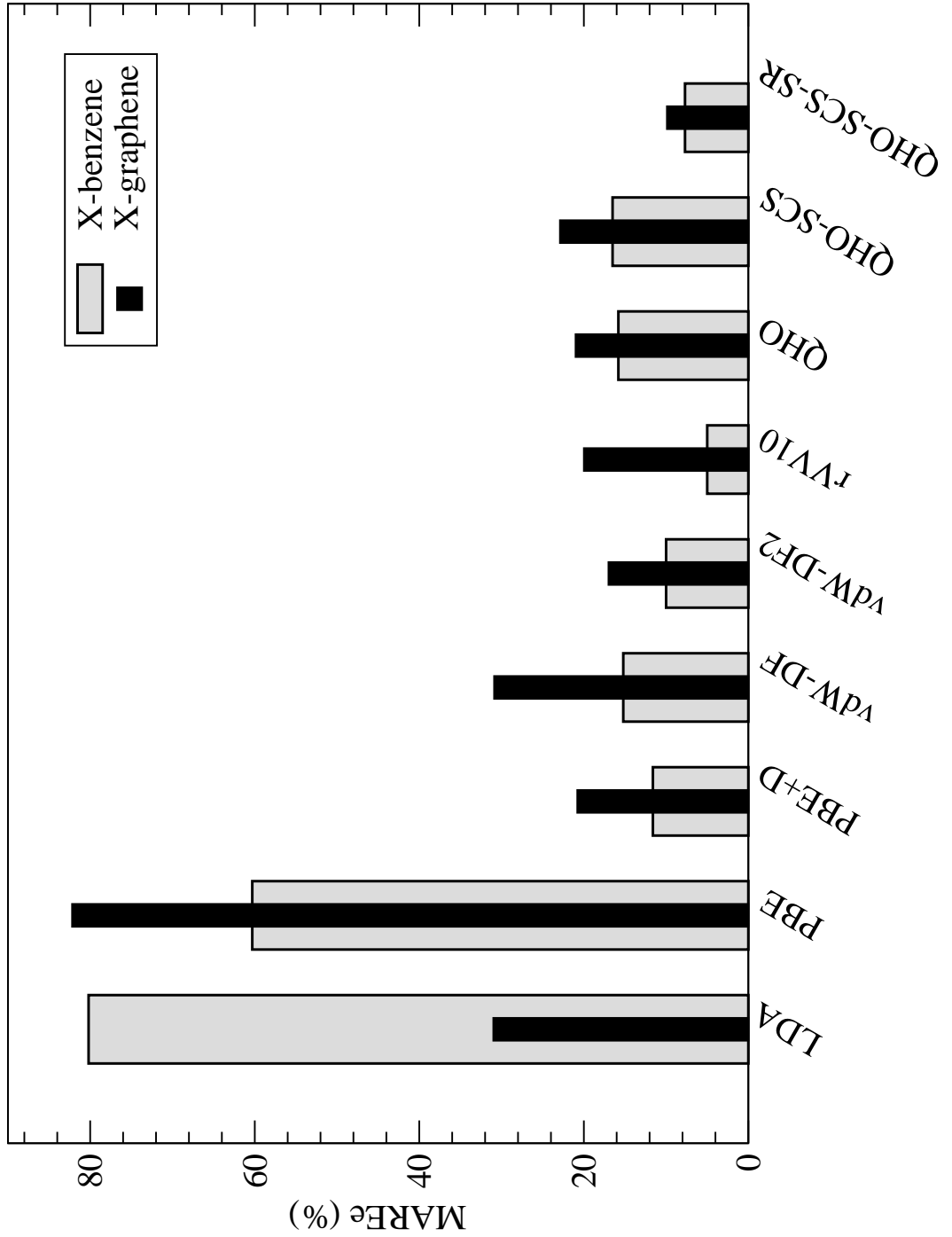


FIG. 1: MARE_e for X-benzene and X-graphene using different methods. For brevity, QHO, QHO-SCS, and QHO-SCS-SR denote the DFT/vdW-QHO, DFT/vdW-QHO-SCS, and DFT/vdW-QHO-SCS-SR methods, respectively.